

Linköping Studies in Science and Technology
Dissertations, No. 1341

Assessment of Myocardial Function using Phase Based Motion Sensitive MRI

Henrik Haraldsson



Linköping University
INSTITUTE OF TECHNOLOGY

Department of Management and Engineering
Department of Medical and Health Sciences
Linköping University, SE-581 85 Linköping, Sweden

Linköping, November 2010

This work has been conducted in collaboration with the Center for Medical Image Science and Visualization (CMIV, <http://www.cmiv.liu.se/>) at Linköping University, Sweden. CMIV is acknowledged for provision of financial support and access to leading edge research infrastructure.

Cover:

DENSE encodes displacement into the phase of the MRI signal. The strength of the displacement encoding gradient in the DENSE acquisition determines the ratio between the displacement and the phase and is chosen to provide a favorable SNR. A side effect of this approach is wrapping of the phase as seen on the cover.

Assessment of Myocardial Function using Phase Based Motion Sensitive MRI

© 2010 Henrik Haraldsson, unless otherwise noted

*Department of Management and Engineering
Department of Medical and Health Sciences
Linköping University
SE-581 85 Linköping
Sweden*

ISBN 978-91-7393-302-5

ISSN 0345-7524

Printed 2010 by LiU-Tryck, Linköping, Sweden

Abstract

Quantitative assessment of myocardial function is a valuable tool for clinical applications and physiological studies. This assessment can be acquired using phase based motion sensitive magnetic resonance imaging (MRI) techniques. In this thesis, the accuracy of these phase based motion sensitive MRI techniques is investigated, and modifications in acquisition and post-processing are proposed.

The strain rate of the myocardium can be used to evaluate the myocardial function. However, the estimation of strain rate from the velocity data acquired with phase-contrast MRI (PC-MRI) is sensitive to noise. Estimation using normalized convolution showed, however, to reduce this sensitivity to noise and to minimize the influence of non-myocardial tissue which could impair the result.

Strain of the myocardium is another measure to assess myocardial function. Strain can be estimated from the myocardial displacement acquired with displacement encoding with stimulated echo (DENSE). DENSE acquisition can be realized with several different encoding strategies. The choice of encoding scheme may make the acquisition more or less sensitive to different sources of error. Two potential sources of errors in DENSE acquisition are the influence of the FID and of the off-resonance effects. Their influence on DENSE were investigated to determine suitable encoding strategies to reduce their influence and thereby improve the measurement accuracy acquired.

The quality of the DENSE measurement is not only dependent on the accuracy, but also the precision of the measurement. The precision is affected by the SNR and thereby depends on flip angle strategies, magnetic field strength and spatial variation of the receiver coil sensitivity. A mutual comparison of their influence on SNR in DENSE was therefore performed and could serve as a guideline to optimize parameters for specific applications.

The acquisition time is often an important factor, especially in clinical applications where it affects potential patient discomfort and patient

through-put. A multiple-slice DENSE acquisition was therefore presented, which allows the acquisition of strain values according to the 16-segment cardiac model within a single breath-hold, instead of the conventional three breath-holds.

The DENSE technique can also be adapted toward comprehensive evaluation of the heart in the form of full three-dimensional three-directional acquisition of the displacement. To estimate the full strain tensor from these data, a novel post-processing technique using a polynomial was investigated. The method yielded accurate results on an analytical model and *in-vivo* strains obtained agreed with previously reported myocardial strains in normal volunteers.

Populärvetenskaplig sammanfattning

Hjärtsjukdomar orsakar mycket lidande och är en av de vanligaste dödsorsakerna i Sverige. För att kunna hjälpa dessa patienter, och även lära mer om de bakomliggande sjukdomarna, så är det viktigt att kunna mäta hjärtats rörelse. En mätteknik som kan användas för att studera rörelsen är så kallad magnetkamerateknik. Denna teknik är inte begränsad till att studera hur hjärtats konturer ändrar sig när hjärtat slår, utan kan även mäta rörelsen inuti hjärtväggen. Tekniken kan även mäta hur snabbt och hur mycket olika delar av hjärtväggen drar ihop sig. Det går därför att studera hur mycket olika delar i hjärtväggen bidrar till hjärtats totala sammandragning. För att på ett bättre sätt kunna ge värdefull information om patienter och ökad kunskap om olika hjärtsjukdomar så behövs dessa mätmetoder förbättras. I denna avhandling presenteras undersökningar om hur dessa mätningar skall utföras för att ge noggranna resultat, hur mätmetoderna kan anpassas till olika användningsområden, samt nya metoder att analysera mätdata. Här följer några korta beskrivningar om de olika arbetena.

Analysmetoden är ett viktigt steg för att studera hur snabbt olika delar av hjärtväggen drar ihop sig. Detta beror på att analysmetoden är känslig för de små osäkerheterna som finns i mätdata. Vi har därför tagit fram en ny analysmetod som är mindre känslig för dessa osäkerheter och som därför ger mer tillförlitliga resultat.

Ett annat sätt att studera hjärtrörelsen är att mäta hur mycket hjärtmuskeln drar ihop sig. Dessa mätningar kan utföras på många olika sätt - det finns många val och prioriteringar. Dessa val kommer bland annat att påverka mätningens noggrannhet. Vi har därför undersökt hur vissa av dessa val gör mätningen mer eller mindre känslig för fel. Vi har även undersökt hur andra av dessa val påverkar mätningens precision. Med denna kunskap kan vi nu bättre anpassa mätningen till olika användningsområden.

Vid mätningar på patienter så är undersökningstiden en viktig aspekt. En kort undersökningstid minskar den oro som vissa patienten upplever i samband med undersökningstiden. Oron kan dessutom leda till försämrade mätresultat i den undersökning som görs. En kortare undersökningstid gör det också möjligt att hinna undersöka fler patienter. Mätmetoden har därför anpassats för att kunna göra en snabb patientundersökning. För att snabba upp mätningen så har vi utnyttjat att magnetkameran ibland har lite väntetid under mätningen. Genom att använda denna väntetid till att mäta på andra ställen i hjärtat så har den totala tiden för mätningen kunnat minska.

För att få mer kunskap om olika sjukdomar så är det många patienter som frivilligt ställer upp på mer omfattande undersökningar. För dessa undersökningar är det viktigt att få en detaljerad och omfattande bild av hur hjärtat drar ihop sig. Mätmetoden och dess analys har därför anpassats till dessa mer omfattande undersökningar. Detta ger oss möjlighet att förstå och förhoppningsvis hitta nya sätt att behandla olika hjärtsjukdomar.

Acknowledgements

During the writing of this thesis, I have had the pleasure of being surrounded by many persons that directly or indirectly have supported me - I owe gratitude to you all.

First of all, I would like to thank Tino Ebbers, my supervisor, for his guidance, support and trust throughout this journey - I hope we both enjoyed the ride.

To my co-supervisor Matts Karlsson, for sharing new ideas and possibilities enthusiastically.

To my co-supervisor Jan Engvall, for providing insights into the clinical routine and patient care.

To my co-supervisor Carljohan Carlhäll, for sharing his interest and knowledge of cardiac physiology.

I would also like to thank all my colleagues in the research group. It has been a pleasure working in the friendly and creative group. I would like to mention: Lars Wigström, for introducing me into the group; Andreas Sigfridsson, for rapid cycles of new ideas, testing and evaluations; Ann Bolger, for sharing her experience and her precise formulations; John-Peder Escobar Kvitting, for providing insights into physiology and cardiac surgery; Petter Dyverfeldt, Jonatan Eriksson and Sven Petersson, for support and constructive advices; Johan Kihlberg, for sharing his knowledge and practical experience of clinical MRI examinations; and Marcel Warn-tjes, for sharing his knowledge of MRI. I would also like to thanks all my colleagues at IMH, IEI, and CMIV.

Finally, I would like to thank all my friends and my family for their continuous support.

Henrik Haraldsson
Linköping, October 2010

Contents

1	Introduction	1
2	Cardiac physiology	3
3	Cardiac mechanics	7
3.1	Assessment of physiological data	8
3.2	Kinematics	9
3.2.1	Strain	10
3.2.2	Strain rate	11
4	Phase based motion sensitive MRI	13
4.1	Basic spin physics	13
4.1.1	Spatial encoding	15
4.2	Motion sensitive MRI	16
4.2.1	Velocity encoded MRI	18
4.2.2	Displacement encoded MRI	19
5	Assessment of myocardial function using MRI	25
6	Aims	27
7	Improving assessment of myocardial function	29
7.1	Improved estimation of strain rate using PC-MRI - Paper I	29
7.2	Influence of the FID and off-resonance effects in DENSE MRI - Paper II	31
7.3	In-vivo SNR in DENSE MRI - Paper III	34
7.4	Multiple-slice DENSE - Paper IV	36
7.5	3D DENSE - Paper V	37

8 Discussion	39
8.1 Possibilities and hindrances of the phase based motion sensitive methods	39
8.2 PC-MRI vs. DENSE	41
8.3 Clinical routine vs. physiological research	42
8.4 Future work	43
Bibliography	45

Chapter 1

Introduction

The number of applications of magnetic resonance imaging (MRI) has grown considerably since its start in the early seventies. One reason for this is that the pulse sequence used in MRI is highly modifiable. The wide range of pulse sequences does not only allow for acquisition of anatomical structures, but also acquisition of different features such as brain activity and diffusion.

This thesis considers the use of MRI for the assessment of myocardial function, and focuses on techniques that use the phase on the MRI signal to measure motion. The papers included in this thesis investigate methods to improve the accuracy and precision of the measurement, adapts the measurement to both research and clinical purpose as well as proposes method for quantification of myocardial function from the data acquired.

The outline of this thesis is as follows: The background of the research area is presented in chapter 2 to 5. It starts in chapter 2 by presenting the basic cardiac physiology. It is the deepening of understanding of cardiac physiology in health and disease that motivates this research. To be able to analyze and describe the function of the myocardium, chapter 3 introduces concepts from mechanics, especially from kinematics. This mechanical framework does however require input data. This leads to chapter 4 which describes MRI and how the phase based motion sensitive acquisitions can be used to study the motion of a beating heart. The chapter presents some of the background information needed to understand the work of the individual papers. The last background chapter provides a survey of previous work within the research area.

Chapter 6 presents the aim of research presented in this thesis while chapter 7 gives an overview of the papers included and also provide some additional reflections related to the individual papers. Finally, chapter 8

provides some general reflection of the research area and its future.

Chapter 2

Cardiac physiology

The heart constitutes of two pumps driving the flowing blood through the systemic and pulmonary system. Oxygenated blood enters the left atrium and continues into the left ventricle which drives the blood throughout the systemic system. The deoxygenated blood returns to the right atrium from which it continues into the right ventricle and into the pulmonary system to be oxygenated again, as illustrated in Figure 2.1.

The pressure difference between the arterial and the venous side of the circulatory system is the main driving force of the blood. This pressure difference, illustrated in Figure 2.2, arises as the heart drives blood by its contraction, supported by the valves which prevent the blood from flowing backward. During diastole, the relaxation of the left ventricle causes its blood pressure to drop. As the pressure drops below that of the left atrium, the mitral valve opens (MVO) and blood will flow from the atrium into the ventricle. Late in diastole, contraction of the atrium increase the atrial pressure that produces a second peak in the ventricular filling. As the ventricle starts to contract in early systole, its pressure rises. When the ventricular pressure exceeds the atrial pressure the mitral valve closes (MVC), preventing leakage back into the atrium. When the rising ventricular pressure exceeds the pressure in the aorta the aortic valve opens (AVO) and blood is ejected from the ventricle into the aorta with a simultaneous increase in the aortic pressure. At early ventricular relaxation, the ventricular pressure starts to drop. When the pressure falls below the aortic pressure the aortic valve closes (AVC); this event occurs at a higher pressure than AVO. Accordingly, the different pumping phases of the cardiac cycle sustain the pressure difference between the arterial and venous side in the circulatory system.

In similarity to other tissues and organs, the heart has the ability to

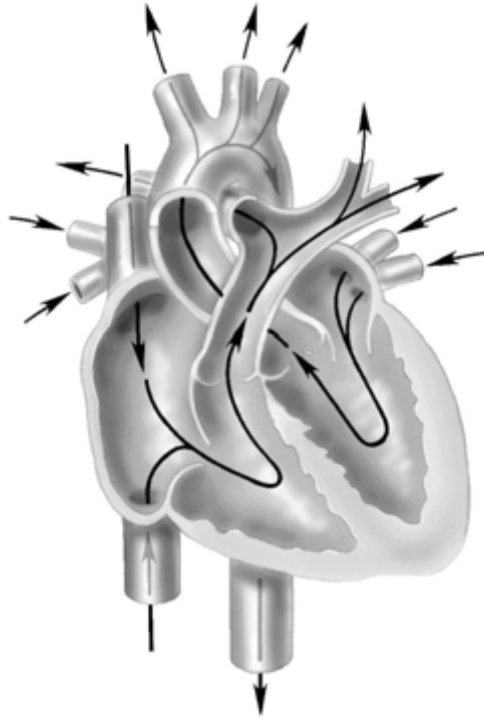


Figure 2.1: The anatomy and blood flow of the heart

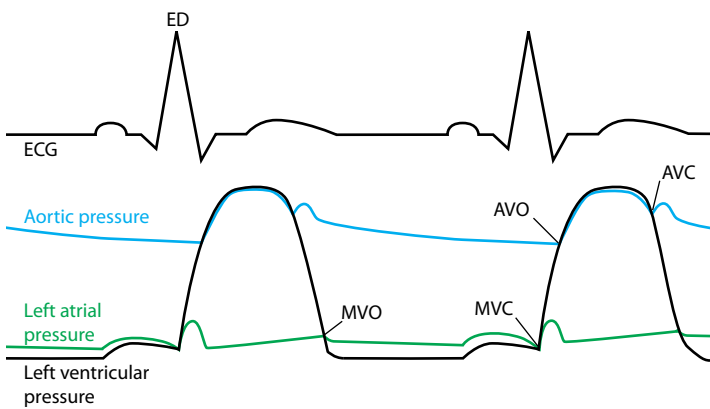


Figure 2.2: ECG and pressure curves of the heart

quickly adapt to various stimuli. In a longer time perspective, the myocardium may also remodel to adapt to its loading conditions. In a healthy heart, remodeling allows endurance athletes to increase their cardiac output and thereby improve their performance. Moreover, remodeling can (for some time) aid to preserve the cardiac output in a diseased heart. Under more chronic conditions, however, the remodeling process can deteriorate the cardiac function. This adverse remodeling may continuously impair the cardiac function eventually leading to irreversible changes. In an attempt to stop this negative trend, various therapies can be used to alter load. The adjusted loading conditions could prevent further deterioration of the cardiac function and even allow for reversed remodeling and restored cardiac function. Two different examples of myocardial remodeling are concentric and eccentric hypertrophy.

Concentric left ventricular hypertrophy is related to a chronic pressure overload. This type of overload may be caused by e.g. high arterial blood pressure or an aortic stenosis which increase the afterload. To adapt to the elevated pressure, the myocardium undergoes hypertrophy; the myocytes become thicker, resulting in increased chamber wall thickness [1]. Eventually there may be fibrosis formation and the myocardium becomes stiff and restricts its own deformation. The concentric hypertrophy is also characterized by decreased longitudinal motion, relative the radial motion, of the left ventricular myocardium [2].

Eccentric left ventricular hypertrophy, on the other hand, is related to a chronic volume overload. This type of overload may be caused by e.g. regurgitant valve disease. To adapt to the increased volume load, the myocardium undergoes hypertrophy; the myocytes become longer, resulting in increased chamber volume [1]. To maintain an adequate stroke volume the dilated chamber has an increased oxygen demand compared to the normal sized chamber, caused by the increased wall tension needed to sustain the pressure in the chamber according to Laplace law.

At an early stage, adverse remodeling of both concentric and eccentric hypertrophy can be reduced or even reversed if the pressure or volume overload is reduced. An early detection of adverse remodeling related myocardial dysfunction is essential to prevent irreversible changes. One such early marker suggested for ventricular dysfunction in mitral regurgitation is alteration of transmural myocardial strain [3]. Measures of deformation, such as strain and strain rate, originate from mechanics and these are used in research and clinic to describe and evaluate cardiac function.

Chapter 3

Cardiac mechanics

In mechanics the term deformation is used for motion which changes the shape of an object, i.e., it describes relative displacement between particles in the object. The regional deformation of the heart is fundamental to fully understand cardiac mechanics as it is the complex sequence of regional deformation that constitutes the contraction and the relaxation of the heart as a whole. In clinical practice, the combined effort of the myocardium is investigated with global measurements. These measurements investigate the cardiac cycle as a whole, e.g. stroke volume, or the timing of the cardiac cycle, e.g. time resolved outflow in the aorta. Global measurements provide valuable information of the general condition of the heart, but they do not reveal the status of specific regions within the myocardium. To gain information of the regional cardiac function requires assessment of the regional deformation.

The relation between the regional deformation, on one hand, and the work of the heart could be described with a generic abstraction of a mechanical problem. This abstraction can be applied on the interaction of the myocardium and the blood, and thereby relate the strain and stress of the myocardium to the volume and pressure of the blood in the chamber. Suppose that the myocytes were triggered which cause a regional contraction of the myocardium. This contraction (*deformation*) leads to a *displacement* of the myocardium which in turn would decrease the volume of the chamber. However, the shrinking chamber volume would increase the pressure (*external forces*) of the blood. Due to the required force balance, the increased pressure results in increased *stress* in the myocardium. Hence, the contraction of the myocardium causes the stress to raise.

Some of the aspects in the abstraction would be difficult to measure directly, for instance the stress of the myocardium within a beating heart.

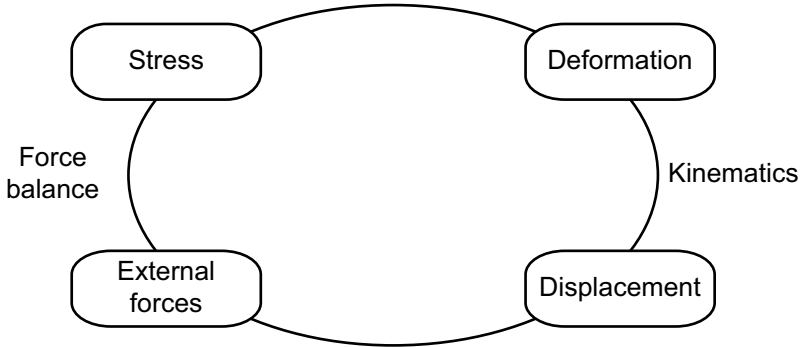


Figure 3.1: Generic abstraction of a mechanical problem

By using the relations given by the mechanical model it could be possible to derive the stress within the myocardium by acquiring the other parameter, e.g. blood pressure, displacement and strain of the myocardium. However, residual stresses, redistributing the stress in the unpressurized tissue, as well as other aspects may complicate this. Hence, a great deal remains to be investigated and learned in this research area. However, even though this approach most likely will be too extensive and computationally demanding for clinical routine it is of great value. Even basic reasoning about cardiac physiology falls back on this abstraction. For example, *a delayed filling of the left chamber may indicate an insufficient supply of oxygen* could be broken down and be explained as: The pressure in the chamber (external force) is approximately normal, and consequently the strain within the myocardium should approximately be normal too. However, due to lack of oxygen the properties in the myocardium are altered which reduce the deformation despite normal stress. This reduction prevents the normal contraction of the myocardial wall that consequently prevents the filling of the ventricle.

3.1 Assessment of physiological data

Evaluation of global or regional cardiac function requires physiological data. It could be data describing the motion, pressure, chemical processes as well as other measurements. There exist a number of different modalities to assess these data. For cardiac applications, the commonly used modalities are; computer tomography, ultrasound, invasive pressure catheters and MRI. Of these modalities, ultrasound and MRI are the ones which are used to assess motion in the myocardium and the blood.

Computer tomography is mainly used to study the geometry of the heart. It provides data with high spatial resolution. This resolution is often utilized to search for narrowed coronary arteries which may cause chest pain and myocardial infarction.

Ultrasound is widely used in clinical routine and has the benefit of being a bedside technique. To measure motion, the technique uses the Doppler effect [4, 5] or speckle tracking [6]. In Doppler measurements, ultrasound can acquire the axial velocity towards or away from the ultrasound probe. Thus, Doppler measurement becomes limited to assess motion along certain directions. This does not to the same extent limit speckle tracking which can track motion perpendicular to the axial direction.

Invasive pressure catheters can be introduced into a large vein and threaded into the heart. The catheter enables accurate measurement of the cardiac blood pressure.

MRI will be described more thoroughly in chapter 4.

3.2 Kinematics

Kinematics is the study of the motion without concerning forces and moments. Continuum mechanics often starts by considering a particle of a body described by its coordinate X_A [7] at time $t = 0$, where $A = \{X, Y, Z\}$. As a particle retains its coordinate X_A independent of movement, X_A is referred to as a material description and describes an reference configuration. Measurement described as a function of this material (reference) configuration is referred to as Lagrangian. The position of this particle at a later time is $x_a = \varphi_a(X_A, t)$, where $a = \{x, y, z\}$. The description of x_a identifies the spatial position of the particle in a deformed configuration. Measurements described as a function of the deformed configuration is referred as Eulerian.

To evaluate deformation on a regional basis one has to describe the motion of a particle in relation to its neighboring particles. In continuum mechanics, this is analyzed with the deformation gradient tensor \mathbf{F} . Written in index notation the deformation gradient tensor is:

$$F_{aA} = \frac{\partial \varphi_a}{\partial X_A} \quad (3.1)$$

The deformation gradient tensor is however sensitive to rigid body motion. This is an unfavorable property for a measure of deformation. Strain, on the other hand, is a measure of deformation unaffected by rigid body motion and is an excellent measure of deformation.

3.2.1 Strain

Deformation of solid tissue is often described in terms of strain. Two suitable properties of strain measures are that *an undeformed state should correspond to zero strain*, and *strain should not change due to rigid body motion*. However, several measures of strain that fulfill these properties exist. Two measures that fulfill these properties and which are commonly used are the Lagrangian strain tensor \mathbf{E} and the Eulerian strain tensor \mathbf{e} .

$$\mathbf{E} = \frac{1}{2} (\mathbf{F}^T \mathbf{F} - \mathbf{I}) \quad (3.2)$$

$$\mathbf{e} = \frac{1}{2} (\mathbf{I} - \mathbf{F}^{-T} \mathbf{F}^{-1}) \quad (3.3)$$

The tensors describe the same deformation, but relate it to different configurations; the Lagrangian strain tensor \mathbf{E} describes the strain in relation to the material (reference) configuration, while the Eulerian strain tensor \mathbf{e} describes it in relation to the deformed spatial configuration. Thus, these two measures are related. The Lagrangian strain tensor can be acquired from the Eulerian strain tensor with the pull-back operator (pb_φ). The pull-back operator transforms the measure describe in relation to the deformed configuration into a measure describe in the reference configuration. The push-forward operator (pf_φ), on the other hand, transforms a measure described in the reference configuration into a measure described in the deformed configuration.

$$\begin{aligned} \mathbf{E} &= pb_\varphi(\mathbf{e}) \\ &= \mathbf{F}^T \mathbf{e} \mathbf{F} \\ &= \mathbf{F}^T \frac{1}{2} (\mathbf{I} - \mathbf{F}^{-T} \mathbf{F}^{-1}) \mathbf{F} \\ &= \frac{1}{2} (\mathbf{F}^T \mathbf{F} - \mathbf{I}) \end{aligned} \quad (3.4)$$

$$\begin{aligned} \mathbf{e} &= pf_\varphi(\mathbf{E}) \\ &= \mathbf{F}^{-T} \mathbf{E} \mathbf{F}^{-1} \\ &= \mathbf{F}^{-T} \frac{1}{2} (\mathbf{F}^T \mathbf{F} - \mathbf{I}) \mathbf{F}^{-1} \\ &= \frac{1}{2} (\mathbf{I} - \mathbf{F}^{-T} \mathbf{F}^{-1}) \end{aligned} \quad (3.5)$$

3.2.2 Strain rate

In solid mechanics, stress is often related to strain. In fluid mechanics, on the other hand, stress in viscous fluids is related to the rate at which the strain change, i.e. strain rate. The strain rate tensor \mathbf{d} is the push-forward of the temporal derivative of the Lagrangian strain, but perhaps more commonly described as the symmetric part of the velocity gradient tensor \mathbf{L} . In index notation the velocity gradient tensor can be written as:

$$L_{ab} = \frac{\partial v_a}{\partial x_b} \quad (3.6)$$

where v_a is the velocity components.

The relation between the strain rate tensor \mathbf{d} and the velocity gradient tensor \mathbf{L} can then be shown as:

$$\begin{aligned} \mathbf{d} &= pf_\varphi \left(\dot{\mathbf{E}} \right) \\ &= \frac{1}{2} \mathbf{F}^{-T} \overline{\left(\mathbf{F}^T \mathbf{F} - \mathbf{I} \right) \dot{\mathbf{F}}} \mathbf{F}^{-1} \\ &= \frac{1}{2} \left(\mathbf{F}^{-T} \dot{\mathbf{F}}^T + \dot{\mathbf{F}} \mathbf{F}^{-1} \right) \\ &= \frac{1}{2} (\mathbf{L}^T + \mathbf{L}) \end{aligned} \quad (3.7)$$

where

$$\begin{aligned} L_{ab} &= \frac{\partial v_a}{\partial x_b} \\ &= \frac{\partial \dot{\varphi}_a}{\partial X_A} \frac{\partial X_A}{\partial x_b} \\ &= \frac{\partial}{\partial t} \left(\frac{\partial \varphi_a}{\partial X_A} \right) F_{Ab}^{-1} \\ &= \dot{F}_{aA} F_{Ab}^{-1} \end{aligned} \quad (3.8)$$

$$\Rightarrow \dot{\mathbf{F}} \mathbf{F}^{-1} = \mathbf{L} \quad (3.9)$$

Chapter 4

Phase based motion sensitive MRI

4.1 Basic spin physics

The fundamental property behind magnetic resonance imaging (MRI) is that of the net nuclear spin [8]. Nuclei with unpaired protons and neutrons have a non-zero net spin. The hydrogen nucleus 1H commonly used in MRI has a spin of $\pm 1/2$. Each of these spins has a magnetic moment vector in the direction of the spin. In an external magnetic field the spin and its magnetic moment vector aligns either with (for spin $+1/2$) or against (for spin $-1/2$) the magnetic field. On a macroscopic level, a group of spin experiencing the same magnetic field strength can be presented as a spin package. As the $+1/2$ spins slightly outnumbers the $-1/2$ spins in room temperature, a spin package produce a magnetic field which could be represented by a magnetization vector. This magnetization vector precesses around the external magnetic field. The Larmor frequency ω with which the magnetization vector precesses is proportional the external magnetic field strength B_0 and to the gyromagnetic ratio γ , specific for the nucleus.

$$\omega = \gamma B_0 \tag{4.1}$$

In a volume, including numerous nuclei, the sum of all magnetization vectors results in a net magnetization M along the external magnetic field, as illustrated in Figure 4.1. At equilibrium, this net magnetization M is referred to as M_0 . The direction of M_0 defines the z -axis and the magnetization along the z -axis is referred to as the longitudinal magnetization. The equilibrium can be disturbed by applying a rotating electromagnetic field, used to nutate the net magnetization along the longitudinal axis onto the

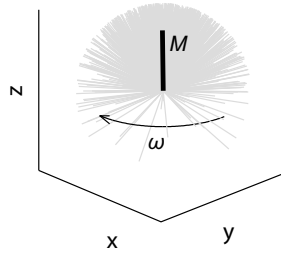


Figure 4.1: The distribution of multiple magnetic vectors (grey) results in a net magnetization M (black). The magnetic vectors precess around the z -axis with the Larmor frequency ω .

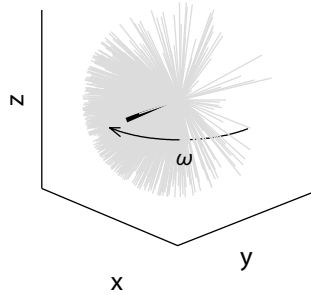


Figure 4.2: The net magnetization is flipped into the transverse plane and rotates around the longitudinal axis with the Larmor frequency ω .

transverse xy -plane. The magnetization vectors continue to precess around the longitudinal axis, thus resulting in a net magnetization which rotates in the transverse plane, as illustrated by Figure 4.2. The electromagnetic signal generated by the rotating net magnetization can be acquired using RF coils; hence, an acquisition of the magnetic resonance, MR.

The net magnetization will over time return to its equilibrium state. The recovery of the longitudinal net magnetization is referred to as T_1 relaxation. For an initial nullified longitudinal net magnetization M_z , the recovery due to the T_1 relaxation is described as a function of time t

$$M_z = M_0 \left(1 - e^{-t/T_1}\right) \quad (4.2)$$

In addition to the longitudinal T_1 relaxation, relaxation also occurs within the transverse plane. This process is referred to as T_2 relaxation. An initial

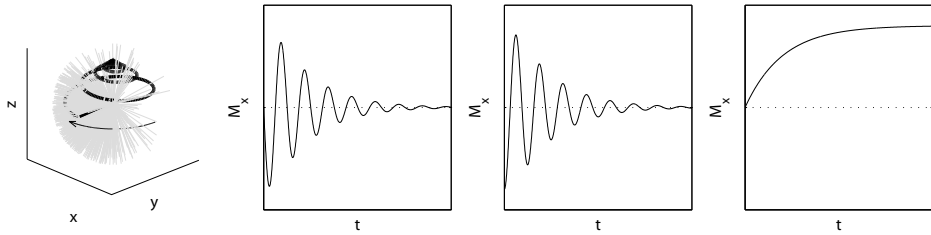


Figure 4.3: The net magnetization regains its equilibrium. The decaying envelope seen for M_x and M_y is the result of the T_2 -relaxation. M_z shows recovery due to T_1 -relaxation.

transverse net magnetization M_{xy0} at time $t = 0$ decays as

$$M_{xy} = M_{xy0}e^{-t/T_2} \quad (4.3)$$

The T_2 relaxation is caused by small deviations in the magnetic field strength attributed to molecular interaction. These deviations in magnetic field strength result in different precession frequency as seen by equation 4.1. The variation in precession frequency dephases the magnetization vectors, and consequently decreases the transverse net magnetization. The deviations attributed to molecular interaction could be referred to as pure T_2 relaxation. This name distinguishes it to dephasing caused by external field inhomogeneities. Relaxation caused by the external field inhomogeneities is referred to as T_2' relaxation. The apparent relaxation caused by the combination of T_2 and T_2' relaxation is called T_2^* relaxation.

$$\frac{1}{T_2^*} = \frac{1}{T_2} + \frac{1}{T_2'} \quad (4.4)$$

Contrary to the pure T_2 relaxation, signal decay caused by T_2' relaxation can be reversed by refocusing the dephased spins. Thus, dependent on the circumstances, the transverse relaxation can range from pure T_2 to T_2^* , or a mixture of them if the T_2' relaxation is only partly regained.

4.1.1 Spatial encoding

MR imaging requires spatial encoding of the MR signal to derive the spatial distribution of the spins. This encoding is achieved in the transverse magnetization by a spatial gradient in the magnetic field strength. This gradient alters the frequency of the precession dependent on position, see equation 4.1. The duration of the gradient and the frequency offset results in phase accumulation. Thus, the magnetic field gradient is used to produce

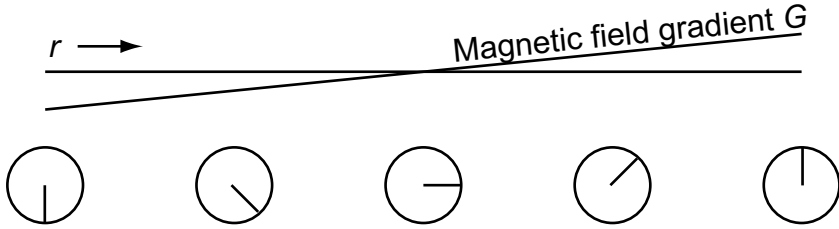


Figure 4.4: A spatial magnetic field gradient produce a spatially varying phase in the transverse magnetization.

a spatially varying phase in the transverse magnetization. The additional phase caused by a gradient lobe G at position r , illustrated in Figure 4.4, could then be written as

$$\varphi(r) = \gamma \int_0^t G(\tau) \cdot r d\tau \quad (4.5)$$

Furthermore, the signal acquired in an MRI experiment is the sum of the transverse magnetization for all positions. The spatial encoding will therefore comply with the Fourier transform [9]. In MRI, the Fourier domain is commonly referred to as k -space, where k describes the spatial modulation of the net magnetization. Analogous to the Fourier transform, the signal acquired in an MRI experiment could be written as

$$s(t) \propto \int M_{xy}(r) e^{-i2\pi kr} dr \quad (4.6)$$

where

$$k(t) = \frac{\gamma}{2\pi} \int_0^t G(\tau) d\tau \quad (4.7)$$

Hence, the MR signal acquired at a certain spatial modulation corresponds to acquiring a sample at the corresponding location in k -space. The basic principle behind MRI is to acquire sufficient of samples in k -space to be able to transform it into an adequate image. However, spatial encoding is not limited to encode images. Spatial encoding of the phase can also be used to encode information of motion into the image.

4.2 Motion sensitive MRI

Most phase based motion sensitive MRI methods can be divided into one of two categorizes; those which utilize the phase of the net magnetization,

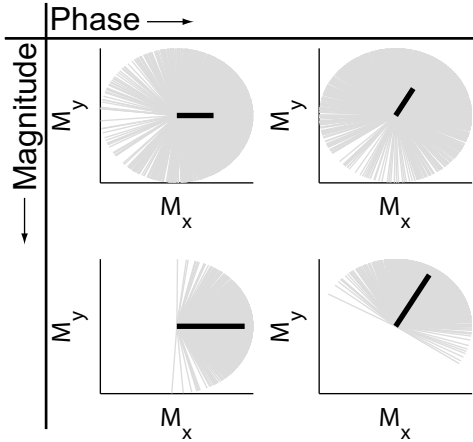


Figure 4.5: The distribution of multiple magnetic vectors can result in different phase and magnitude of the net magnetization.

and those which utilize the altered magnitude due to rearrangement of the spins.

The first category includes techniques to study bulk motion. For ideal bulk motion, all adjacent magnetic vectors experience similar position encodings. The phase of the adjacent magnetic vectors is therefore relatively homogeneous, and consequently the magnitude of the net magnetization becomes relatively large. Depending on the acquisition technique, the phase of the net magnetization can be encoded to contain information of the displacement [10] or velocity [11] of these adjacent magnetic vectors. However, as the net magnetization is the sum of numerous adjacent magnetic vectors, the phase is limited to depict the mean motion of these adjacent magnetic vectors.

If the first category emphasize the homogeneity of the magnetic vectors to study bulk motion, the second category emphasize the heterogeneity of the adjacent magnetic vectors to study their relative difference in motion. This relative difference may be caused by diffusion [12] or turbulence [13]. It causes the magnetic vectors to experience different position encodings, thereby widening the range of phases among the adjacent magnetic vectors. As a result, the magnitude of the net magnetization decreases for heterogeneous motion. Hence, depending on the acquisition technique, diffusion or turbulence causes a drop in net magnetization unrelated to the bulk motion.

The following two sections will describe how the phase of the net magnetization could be used to acquire velocity and displacement data.

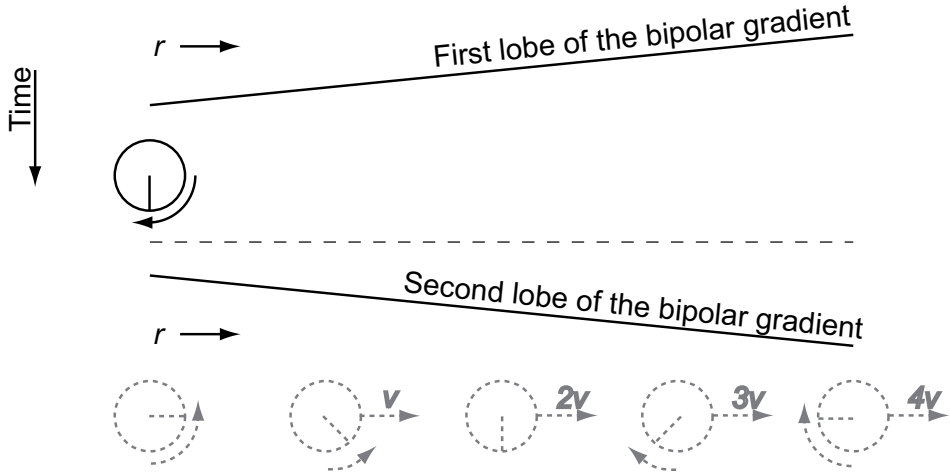


Figure 4.6: For stationary spins the phase acquired in the first lobe of the bipolar gradient are rewound by the second part. The phase is not rewound for moving spins. The accumulated phase is proportional to the velocity of the spins, as illustrated by the spins moving with four different velocities.

4.2.1 Velocity encoded MRI

In phase contrast MRI (PC-MRI) the velocity is encoded into the phase of the spins with a bipolar gradient. The bipolar gradient could be described as two consecutive position encodings performed in opposite direction. The two lobes of the bipolar gradient have the same position encoding strength. The phase in stationary tissue will therefore ideally experience two counteracting position encodings, and are therefore unaffected by the bipolar gradient. Moving tissue, however, will be located at different positions during the two lobes of the bipolar gradient. The two position encodings will therefore not cancel out, resulting in a phase accumulation proportional to the velocity.

The bipolar gradient is unfortunately not the only contributor to the phase. Deviation from the ideal on-resonance frequency also accumulates phase. The off-resonance frequency results from chemical shift and magnetic field inhomogeneities. To prevent this influence, PC-MRI includes an additional velocity encoded acquisition that serves as a phase reference. Measurement of three velocity components and its relation to off-resonance requires four acquisitions. The phase of these four acquisitions, φ_1 to φ_4

can be described as

$$\begin{bmatrix} \varphi_1 \\ \varphi_2 \\ \varphi_3 \\ \varphi_4 \end{bmatrix} = \begin{bmatrix} M_{1x} & M_{1y} & M_{1z} & 1 \\ M_{2x} & M_{2y} & M_{2z} & 1 \\ M_{3x} & M_{3y} & M_{3z} & 1 \\ M_{4x} & M_{4y} & M_{4z} & 1 \end{bmatrix} \begin{bmatrix} v_x \\ v_y \\ v_z \\ \Delta\phi_{off} \end{bmatrix} \quad (4.8)$$

v_x , v_y and v_z are the velocities in three orthogonal directions, and $\Delta\phi_{off}$ is the phase accumulated due to frequency off-resonance. The components $M_{..}$ describe the first order moment of the bipolar gradient along a certain direction, e.g. M_{1x} describe how the velocity along the x direction influence the phase in the first acquisitions. Given the phase in the four velocity encoded acquisitions, equation 4.8 have to be solved to obtain information of the velocities. Two common velocity encoding strategies in PC-MRI are the simple four point method [14]

$$\begin{bmatrix} \varphi_1 \\ \varphi_2 \\ \varphi_3 \\ \varphi_4 \end{bmatrix} = \begin{bmatrix} -M & -M & -M & 1 \\ +M & -M & -M & 1 \\ -M & +M & -M & 1 \\ -M & -M & +M & 1 \end{bmatrix} \begin{bmatrix} v_x \\ v_y \\ v_z \\ \Delta\phi_{off} \end{bmatrix} \quad (4.9)$$

and the Hadamard encoding [15].

$$\begin{bmatrix} \varphi_1 \\ \varphi_2 \\ \varphi_3 \\ \varphi_4 \end{bmatrix} = \begin{bmatrix} -M & -M & -M & 1 \\ +M & +M & -M & 1 \\ +M & -M & +M & 1 \\ -M & +M & +M & 1 \end{bmatrix} \begin{bmatrix} v_x \\ v_y \\ v_z \\ \Delta\phi_{off} \end{bmatrix} \quad (4.10)$$

As described, PC-MRI encodes velocity into the phase of the MR signal. However, phase is modulus arithmetics, and the velocity is therefore cyclically mapped to the phase, a problem referred to as phase wrapping. Thus, the velocity is not uniquely mapped to phase. A common approach to alleviate this problem is in PC-MRI to choose sufficiently low velocity encoding gradient to prevent ambiguities within the expected range of velocity. For example, for the flow in the aorta $v_{max} \approx 2 - 1m/s$ [16, 17, 18, 19, 20], for flow in the heart $v_{max} \approx 1.0 - 0.6m/s$ [21, 22, 23, 24] and for the myocardium $v_{max} \approx 0.3 - 0.1m/s$ [25, 26, 27, 28, 29, 30, 31].

4.2.2 Displacement encoded MRI

In velocity encoding, two consecutive position encodings are used to acquire the velocity. These are performed consecutively to acquire the displacement during a very short time interval, used to produce a good estimate of the

velocity. Displacement encoding MRI, on the other hand, is used to study displacement over a longer time interval. The two position encodings are therefore further separated in time. The first position encoding constitutes an encoding of a reference configuration and corresponds to the starting point of the motion. The second position encoding corresponds to the ending point of the motion and position encodes the deformed configuration. This second position encoding immediately precedes the MRI readout. The time between these two position encoding is commonly in the order of hundreds of milliseconds, significantly longer than for velocity encoding. To allow for the extended time between the two positions encoding the data is commonly acquired using stimulated echo acquisition mode (STEAM) [32, 33].

For a stimulated echo, the initially position encoded magnetization is restored along the longitudinal axis. Along this axis it is exposed to the T_1 relaxation instead of the T_2 relaxation that would have effected the magnetization if it were to reside in the transverse plane. As the T_1 relaxation is slower than the T_2 relaxation, the stimulated echo allows for a prolonged time between the two position encodings. Before the readout, parts of the signal once again has to return to the transverse plane. The acquisition used to acquire the displacement encoded stimulated echo consists of three RF pulses. The initial position encoding preparation is shown in Figure 4.7. This preparation is shared for MRI techniques such as Displacement encoding with stimulated echo (DENSE) [10] and 1-1 SPAMM tagging [34], which both is used to study motion. However, the stimulated echo is not the only signal component resulting from the initial position encoding preparation. Two addition signal components will appear; a stimulated anti-echo and a FID.

Phase modulation in the spatial domain corresponds to two peaks in the frequency domain; hence, there are two stimulated echoes producing two off-center peaks in k -space. These two peaks decay over time due to the T_1 relaxation and are recovered as an unmodulated signal component at the center in k -space. Hence, the STEAM acquisition results in three signal components; two spatially encoded stimulated echoes which originates from the initial position preparation, and one un-encoded FID which originates from the T_1 recovered spins, as illustrated by Figure 4.8.

The three peaks in k -space can be read out once or multiple times. In DENSE, which is the main focus of this section, a second position encoding (referred to as position decoding) has to be performed before each of the readouts, as shown in Figure 4.9. The second position decoding gradient shifts the center of k -space so that at the stimulated echo resides in the

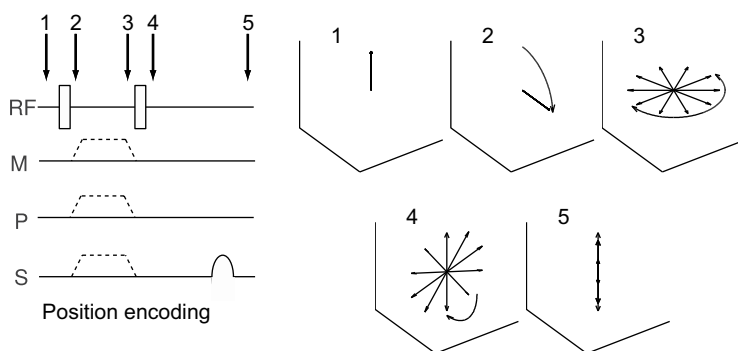


Figure 4.7: Initial position encoding shared for DENSE and 1-1 SPAMM tagging.

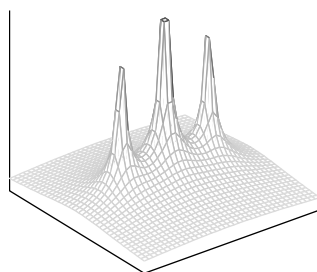


Figure 4.8: Three peaks in k -space. The FID (the center peak) originates from T_1 recovered spins. The other two peaks originate from the SPAMM modulation.

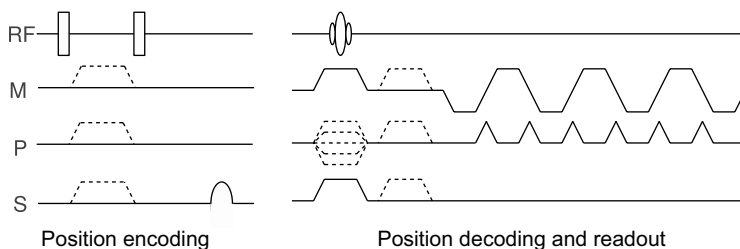


Figure 4.9: DENSE acquisition

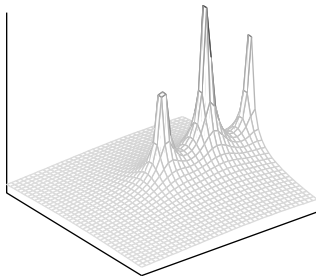


Figure 4.10: Three peaks in k -space shifted by the second position encoding gradient.

center (Figure 4.10). The signal acquired during readout can be written as

$$\begin{aligned}
 M_{xy} = & \underbrace{\frac{1}{2} M e^{i\gamma k \delta + i(S_2 - S_1) + i\theta} e^{-t/T_1}}_{\text{Stimulated echo}} + \\
 & \underbrace{M_0 \left(1 - e^{-t/T_1}\right) e^{i(\gamma k r_2 + S_2)}}_{\text{FID}} + \\
 & \underbrace{\frac{1}{2} M e^{-i\gamma k \delta + i(2\gamma k r_2 + S_2 + S_1) - i\theta} e^{-t/T_1}}_{\text{Stimulated anti-echo}} \quad (4.11)
 \end{aligned}$$

where M is the magnetization prior to the first RF pulse, M_0 is the thermal equilibrium of the z-magnetization, k describe the strength of the displacement encoding gradients, δ is the displacement of the studied subject, and θ is the phase of the second RF pulse. The phase contribution due to off-resonance during position encoding and position decoding is denoted S_1 and S_2 respectively.

As it is the phase of the stimulated echo that is used for displacement encoding, the other two signal components could be considered to be artifact generating signal components. These artifact generating components have been suppressed with different techniques; inversion recovery [35], k -space filters [36], the choice of in- and through-plane decoding [10, 35, 37], and RF phase cycling [38, 39, 40]. In RF phase cycling, different linear combinations of the three signal components can be acquired by cycling the phase θ of the second RF pulse. This could suppress one [41, 38] or two [39, 42] of the signal components from equation 4.11. Phase cycling is performed for each of the encoding directions independently.

$$M_{xy|\theta=0} - M_{xy|\theta=\pi} = \underbrace{M e^{i\gamma k\delta + i(S_2 - S_1)} e^{-t/T_1}}_{\text{Stimulated echo}} + \underbrace{M e^{-i\gamma k\delta + i(2\gamma k r_2 + S_2 + S_1)} e^{-t/T_1}}_{\text{Stimulated anti-echo}} \quad (4.12)$$

$$\frac{2}{3} M_{xy|\theta=0} + \frac{2}{3} e^{-i2\pi/3} M_{xy|\theta=2\pi/3} + \frac{2}{3} e^{i2\pi/3} M_{xy|\theta=-2\pi/3} = \underbrace{M e^{i\gamma k\delta + i(S_2 - S_1)} e^{-t/T_1}}_{\text{Stimulated echo}} \quad (4.13)$$

As seen in equation 4.13, RF cycling can be used to acquire the displacement encoded stimulated echo. However, the equation also shows that the phase of the stimulated echo is dependent on both the displacement and phase accumulated due to off-resonance. Analogous to velocity encoding, phase based displacement encoding commonly includes an additional encoding direction to take the off-resonance influence of the phase into account. The encoding scheme could be described analogous to equation 4.8.

$$\begin{bmatrix} \varphi_1 \\ \varphi_2 \\ \varphi_3 \\ \varphi_4 \end{bmatrix} = \begin{bmatrix} D_{1x} & D_{1y} & D_{1z} & 1 \\ D_{2x} & D_{2y} & D_{2z} & 1 \\ D_{3x} & D_{3y} & D_{3z} & 1 \\ D_{4x} & D_{4y} & D_{4z} & 1 \end{bmatrix} \begin{bmatrix} d_x \\ d_y \\ d_z \\ \Delta\phi_{off} \end{bmatrix} \quad (4.14)$$

Moreover, displacement encoding suffers from phase wrapping. For velocity encoding the common approach is to choose a suitable gradient strength to avoid these wraps. However, these wraps are not as problematic for displacement encoding as it is for velocity encoding. Displacement is commonly used to study tethering solid tissue, in which sudden changes of displacement are rare. The phase is therefore slowly varying within the connected tissue, enabling unwrapping of the phase, as illustrated in Figure 4.11. This unwrapping of the wrapped phase is needed to acquire displacement maps. However, to calculate strain maps it is sufficient with a regional unwrapping of the phase as strain relates to the spatial variation of the displacement.

Contrary to PC-MRI, phase wrapping seldom limit the encoding gradient for DENSE acquisitions. The encoding strength is instead often limited by the signal loss caused by compression of the tissue [43]. This loss is caused by the increased heterogeneity in phase of adjacent magnetic vectors in the deformed tissue. Hence, the displacement encoding strength should

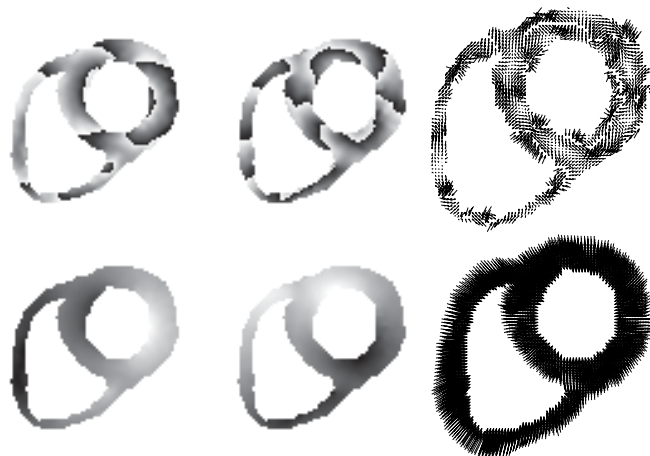


Figure 4.11: The top row shows the wrapped phase and the corresponding arrow plot whereas the bottom row show the unwrapped counterparts.

be chosen with respect to the expected deformation of the tissue to ensure sufficient signal [44].

Chapter 5

Assessment of myocardial function using MRI

Quantitative evaluation of myocardial function is often based on the ideas of spatial modulation of magnetization [34] or of cine phase contrast [45]. These two basic ideas can be modified for different purposes and several approaches to utilize their output have been presented.

In resemblance with tissue Doppler acquisition, PC-MRI can be used to evaluate the myocardial function based on the velocities acquired. PC-MRI velocity data allow acquisition of velocity in all directions and does thereby enable different ways to analyze the data compared to tissue Doppler acquisition. PC-MRI has for instance been used to evaluate myocardial function from the twist of the myocardium [46], and has also been used to provide comprehensive time-resolved survey of the different velocity components in different regions of the heart using a 3D acquisitions [47].

The PC-MRI acquisition can be adapted for different features. The high temporal resolution of the tissue Doppler acquisition has encouraged approaches to acquire the velocity with high temporal resolution using MRI. The pursuit of high temporal resolution have lead to approaches were the different encoding directions are acquired in consecutive cardiac cycles combined with view-sharing, that samples the central k -space more frequently, combined and with double navigator-gating [48].

The muscle fibers in the myocardium constitute a complex interconnected tissue. This tethering connection causes myocardium with impaired function to follow its surrounding, and may thereby make it difficult to differentiate the velocity in tissue with impaired function from healthy tissue. To separate active and passive motion in the myocardium, the velocities from PC-MRI can be used to estimate strain rate [49]. The method used to

estimate strain rate from PC-MRI range from dedicated approaches that estimate the transmural gradient in the myocardium to obtain a single strain rate component [27] to broad approaches that acquire the full strain rate tensor from a 3D acquisition [50]. Strain rate can also be acquired by altering the PC-MRI acquisition to measure the through-plane strain rate directly [51].

The time resolved velocity data acquired with PC-MRI can also be used to track imaginary particle, an approach that especially has been utilized for particle tracing in blood flow [21]. However, particle tracing can also be used in the myocardium where the cyclicity of the myocardium can be exploited through the use of Fourier based cyclic intergration [25]. These myocardial particle traces allows for estimation of regional strain within the myocardium [52] as well as estimate measures on a larger scale [31]. Tracking of the myocardium can also be combined with regularization to obtain a more robust tracking [53].

Not only PC-MRI, but also spatial modulation of the magnetization enables different approaches to acquire and evaluate myocardial function. The spatial modulation of magnetization can produce tagging patterns to study motion [34] and allows for finite analyze of the myocardial strain [54]. To avoid tedious tag-line-tracking, two approaches has been suggested to obtain the displacement from a SPAMM like acquisition directly; DENSE [10] and HARP [55]. The basic ideas behind these techniques are similar and has even been presented as *two views on the same technique of phase-based strain imaging* [56]. The difference between the two techniques is that while HARP is a post processing technique for SPAMM-tagged acquisitions, DENSE could be described as a modification of a SPAMM pulse sequence. Both SPAMM-tagging and DENSE acquisition have been used mainly to study myocardial function based on 2D slices. However, both techniques can be performed with 3D acquisitions [57, 58] and can be used to study other tissues as well. Displacement encoding has for instance been used to evaluate strain in the common carotid artery [59] and the displacement in the cardiac-synchronized brain motion [60, 61]. DENSE has also been combined with PC-MRI to non-invasively acquire regional viscoelastic parameters of the myocardium [62].

Similar to how a modification of PC-MRI can be used to acquire strain rate directly, a modification of SPAMM-tagging can be used to directly acquire through-plane strain in the myocardium [63].

Chapter 6

Aims

The aim of the research described in this thesis was to evaluate and improve quantitative methods for the assessment of myocardial function using phase based motion sensitive MRI. Specific aims addressed in this thesis are:

- Evaluate data acquisition to enable improved measurement accuracy and precision
- Refine the acquisition strategy for research as well as clinical purposes
- Enhance post-processing techniques for the quantification of myocardial function from the data acquired

Chapter 7

Improving assessment of myocardial function

This chapter mainly summarize the papers included in this thesis, but also provides some additional comments and preliminary data not included in the papers.

7.1 Improved estimation of strain rate using PC-MRI - Paper I

Investigation of diastolic and systolic dysfunction of ischemic heart can be facilitated by improved estimation of strain rate. Strain rate has previously been measured with both ultrasound and PC-MRI. For ultrasound, the velocity acquired with the tissue Doppler technique allows to produce strain rate estimates with high temporal resolution. However, as tissue Doppler only allows for acquisition of the velocity along the axis of the beam this technique is limited to acquire strain rate along this axis. Speckle tracking, a more recent method to analyze ultrasound images, is not hampered by this limitation as it allows for estimation of velocities perpendicular to the beam. This technique has also been suggested to acquire strain rate in the non-axial directions [6].

Strain rate has also been estimated from velocity data acquired with PC-MRI [49, 64]. For PC-MRI, signal from blood flowing through the image slice is a potential cause of artifacts during acquisition of myocardial velocity. The high signal intensity of the inflowing blood and the natural variation of the inflow between cardiac cycles affect the k -space lines inconsistently. Consequently, this may result in an artifact which appears as ghosting in the phase-encoding direction. Presaturation of the inflow-

ing blood has been suggested to suppress this artifact for measurements of myocardial velocity [26].

Given the PC-MRI velocity data, different methods to calculate the strain rate have been proposed. Some of these methods are used to estimate a single strain rate component, e.g. estimating the radial strain rate component as the transmural gradient of the radial velocity [27, 65], while other suggested estimation of the full in-plane strain rate tensor. This tensor has been estimated as the finite differences in the velocity between neighboring pixels [49, 64]. Finite differentiation is however sensitive to noise which may deteriorate the strain rate estimates. Low pass filtering of the acquired velocity field could be used reduce this noise. However, a side effect of the low pass filtering is that it would impair the strain rate estimates close to the border of the myocardium as the filter would incorporate velocities from tissue adjacent to the myocardium. To deal with this problem, Paper I proposes the use of normalized convolution to estimate strain rate from PC-MRI. Normalized convolution estimates the velocity gradients using the acquired velocity in conjunction with a myocardial mask. This allows for estimation of the velocity gradients with an adaptable filter kernel which automatically varies size according to the mask. It thereby prevents the filter kernel to include data outside the myocardial mask, thus restricting velocities of the non-myocardial tissue near the endo- and epicardium to influence the estimates. The evaluation of the method is performed on a synthetic velocity dataset and on *in-vivo* data acquired from one healthy volunteer and from one patient with a prior anteroseptal transmural infarction. The synthetic dataset allowed comparison of different methods to derive strain rate tensors from the velocity field with analytically computed strain rate tensors. The analysis of the synthetic dataset showed that normalized convolution could address the problem with noise while at the same time preventing the velocities outside the myocardium to impair the strain estimation. Paper I further demonstrates the feasibility of the method *in-vivo*. For the *in-vivo* measurements, the signal from inflowing blood was suppressed to reduce the inflow ghosting artifact. This saturation was achieved by two spatial saturation pulses placed at each side of the measured slice. This suppression of the signal of the blood was not only important to suppress the ghost artifact, but also to produce sufficient contrast between the myocardium and blood to allow for the segmentation needed to generate the mask applied in the normalized convolution. The saturation was performed for every TR to maintain the saturation of the blood for all time frames. A flip angle of 45 degree for the saturation pulses was experimentally found to be sufficient to maintain the saturation while

at the same time lower the SAR compared with the standard 90 degree flip angle. The time resolved PC-MRI images allowed for segmentation of the myocardium, and the strain rate estimation using normalized could be applied and showed low strain rate in regions with late contrast enhancement indicating non-viable myocardium.

The primary practical difficulty with using normalized convolution to acquire strain rate *in-vivo* was found to be the segmentation. Even though the saturation of the inflowing blood improved the contrast between the myocardium and the blood, some of the time frames still suffered from low contrast. The insufficient saturation was probably caused by slow-flowing blood close to the endocardial border. This effect may be more prominent in patient with perturbed flow. Other segmentation techniques may be less sensitive to the reduced contrast, and a segmentation tool adapted to this specific use should be feasible.

7.2 Influence of the FID and off-resonance effects in DENSE MRI - Paper II

DENSE is a quantitative method. As such it should ideally be independent of its implementation and the measurement system. Any such dependence would diminish the diagnostic value of the measurement and method. DENSE allows for different encoding strategies, something which could be seen in the field. Methodological studies evaluating the effects of differences in the implementation of DENSE could therefore benefit both the clinical diagnostic and studies of cardiovascular physiology.

The DENSE acquisition results in three signal components. Of these signal components the FID and the simulated anti-echo could be considered to be artifact generating signal components. Multiple methods exist to suppress these artifact generating signal components; inversion recovery [35], k -space filters [36], the use of strategic displacement-encodings to separate the signal components [10, 35, 37], and RF phase cycling [38, 39, 40]. For another MR application utilizing stimulated echo acquisition, a study has been performed to investigate the main field inhomogeneities influence on the data acquired [66]. That study showed that a quadrature combination of phase shifted acquisitions may reduce this inhomogeneity dependency. Furthermore, the study points out that a delay of the readout causes the measurement to become sensitive to T_1 -recovery. The purpose of Paper II was to evaluate how the choice of phase reference in DENSE effected the influence of the FID and off-resonance effects.

One of the difficulties with methodological evaluations of clinical meth-

ods is the lack of reliable reference data *in-vivo*. Paper II therefore included two parts; a phantom study and an *in-vivo* study. The phantom study provided a reliable reference, i.e. zero displacement and strain, which allowed the study of the effects in absolute values. For the *in-vivo* study, described more in detail later, multiple slightly altered measurements were performed for each of the different implementations of the DENSE acquisition. The alterations were designed to affect the phase of the FID and performing the measurements with both on- and off-resonance frequency. Neither the FID or off-resonance effects should ideally influence the measurements; thus, deviating results among the acquisitions would show influences of the FID or the off-resonance effects.

To study the FID's influence on the DENSE acquisition, measurements with different phase of the second RF pulse were performed. These measurements can be combined in different ways to produce displacement data. One of these combinations results in a 45 degree phase shift of the FID. Measurements performed on a stationary phantom would therefore ideally result in a 45 degree difference in the phase of the FID and the displacement encoded stimulated echo. As the FID should not influence the DENSE measurement these 45 degrees should ideally not affect the acquired displacement data. For DENSE implementations undesirably influenced by the FID, the increasing signal strength of the FID and decreasing signal strength of the stimulated echo would produce a temporally varying phase in the acquired data and thereby reveal the influence of the FID. This approach could not be used for *in-vivo* measurements as the phase will vary due to the motion of the heart. Instead, the *in-vivo* evaluation was performed by combining the *in-vivo* data in two different way differing in the resulting phase of the FID. These two combinations would ideally provide identical displacement data as long as they were unaffected by the FID. The results of these experiments imply that the use of an encoded phase reference is to prefer over an un-encoded phase reference.

To study off-resonance, a stationary phantom was constructed containing regions with two different Larmor frequencies; one on-resonance consisting of a gelatin mixture and one off-resonance consisting of fat. For both of the regions, deviation from the ideal zero displacement in this stationary phantom indicates measurements inaccuracy. Furthermore, different result between the two regions would indicate that off-resonance effects influence the DENSE measurements. The influence off-resonance effects was also evaluated *in-vivo*. For this *in-vivo* evaluation the measurements itself were performed with three different frequencies; one on-resonance and two off-resonance. The frequency offset used in the two off-resonance measure-

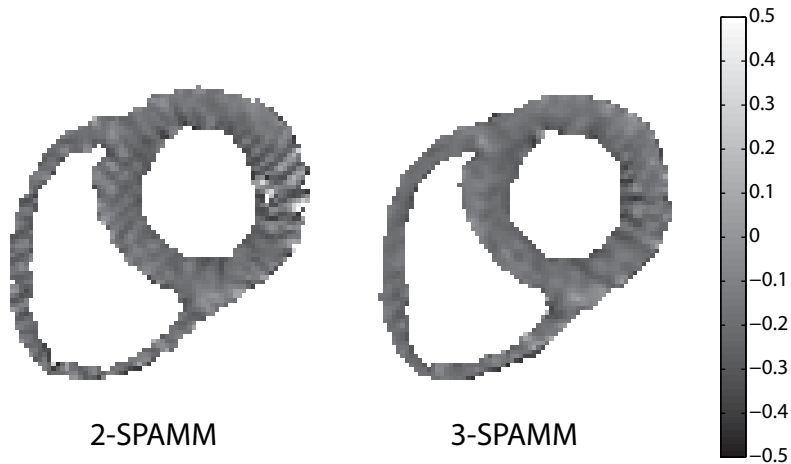


Figure 7.1: Contraction of the heart illustrated by the low eigenvalue of the Lagrangian strain tensor. The left plot shows the strain calculated from 2-SPAMM while the right plot is calculated from 3-SPAMM.

ments were kept within a clinically relevant range. The result implied that the use of a displacement encoded reference or the use of a complementary reference was less influenced by the frequency offset.

Based on the result on Paper II, the use of a displacement encoded phase reference is preferred as this seems to reduce the influence of both the FID and the off-resonance effects at a small price. In addition to what is discussed in Paper II, it is worth to mention that the use of RF cycling technique like the use of quadrature combined data seem advantageous in other aspects. The principle behind the RF cycling could be seen as a generalized SPAMM approach in terms of a N -SPAMM encoding [42]. N -SPAMM uses N evenly distributed phases of the RF pulse per encoding direction. In this manner N equal to 2 correspond to CSPAMM [41] and N equal to 4 is related to CANSEL [39]. Using N greater than 2 allows for suppression of both artifact generating echoes. A preliminary comparison of 2- and 3-SPAMM shows that 3-SPAMM in practice seem successful in suppressing the zebra-stripe artifacts. It is especially interesting to compare its effect the derived strain, as illustrated in Figure 7.1.

The result presented in Paper II is mainly dealing with the accuracy of the DENSE measurement.

7.3 In-vivo SNR in DENSE MRI - Paper III

The analysis and interpretation of the acquired data are in general dependent on SNR. MRI is no exception to this and it is important to obtain sufficient MR signal to obtain clinically useful examinations. The need for high SNR may especially be true for quantitative measurements. The human vision is capable of extracting information from noisy images, a feature that allows us to perceive anatomical structures despite low SNR. In computer based quantitative analysis, however, it may be a difficult task. The data analysis itself may furthermore lower SNR compared with the input data, as is the case with strain estimation from displacement data. This accentuates the importance of SNR for DENSE acquisitions.

DENSE is based on the stimulated echo and does consequently exhibit an intrinsic 50% signal loss. The remaining 50% decays during the cardiac cycle due to the T_1 -relaxation. This limits the available signal throughout the cardiac cycle. The T_1 -recovered spins in DENSE, contrary to conventional cine imaging, do not contribute to the signal of interest until the next displacement encoding preparation is performed in the beginning of the succeeding cardiac cycle. It is therefore also important to consider that a too greedy data acquisition, acquiring more time frames than needed for the application at hand, may come at a high price in terms of lower SNR. Moreover, the signal may also be reduced by intravoxel phase dispersion caused by the deformed tissue [43]. All these inherent effects of the DENSE acquisition promote thoughtful acquisition of displacement data; however, SNR can be increased by several means. These are often related to trade-offs. To be able to find the appropriate choice for the application at hand a comparative study of these methods is necessary.

Previous studies about SNR in DENSE-like techniques are mainly found for SPAMM tagging. These techniques do more or less use the same spatially modulated preparation to encode position into the magnetization. One approach proposed for SPAMM tagging acquisition is the use of a dynamic flip angle to obtain constant SNR throughout the cardiac cycle [67], an approach also applied for DENSE acquisition. This approach can further be optimized with regards to T_1 -relaxation and heart rate to increase the beat-to-beat steady-state magnetization [68].

Another aspect which influences the SNR for DENSE and SPAMM is the magnetic field strength. For tagging, previous studies have compared the difference between 1.5T and 3T in terms of contrast-to-noise for the tag-lines [69, 70, 71, 72].

The aim of Paper III was to perform a mutual analysis of different possibilities to increase the SNR: flip angle strategies, field strength and

spatial variation of receiver coil. In addition to the individual results the mutual comparison provides additional value as the influence of the different approaches was compared in the same or a similar setting. It could therefore serve as a support in the decision of how to achieve sufficient SNR.

Ten healthy volunteers were examined on 1.5T and 3T with different excitation patterns, flip angle strategies and coils. The SNR of these measurements was investigated using per-pixel estimates [73, 74] from which the average SNR in a proximal and a distal region of the left ventricle could be calculated. The results of the study showed that all of the following changes resulted in an approximately 50% increase in SNR; changing from a magnetic field strength of 1.5T to 3T ($53 \pm 26\%$), going from a distal region to a proximal ($59 \pm 26\%$), and changing a 5/6-channel coils with a 32-channel coils ($52 \pm 29\%$). An interesting reflection based on this result is that the higher magnetic field strength and the greater coil coverage produced the same increase in SNR, they are however expected to differ substantially in terms of economical investment. This reflection should of course also be seen in the light of other advantages and disadvantages of the use of higher field strength. Furthermore, the result also showed that the use of a greedy approach, by acquiring a full cine DENSE acquisition while only needing a single end systolic time frame may be very costly. The single time frame acquisition provided a three-fold increase in SNR for a fixed flip angle compared to the cine acquisition. The increase was even larger for the flip angle optimized for constant SNR, in which case the increase was six-fold. This result points out the importance of deciding the data analysis in advance, as acquiring cine data while in retrospective only analyze a single time frame comes at a high price.

Beyond the scope of Paper III, a comparison of an alternative k -space trajectory has also been investigated. The preliminary results indicate an approximate three-folded improvement in SNR with the use of a segmented spiral readout instead of an interleaved k -space segmented EPI readout. These two acquisition methods were however performed with different t-factors and timings which should be taken into consideration. A possible limitation of this preliminary comparison is that parts on the per-pixel analysis may be sensitive to the non-white noise expected for spiral acquisitions. Its effect has however not been further investigated and should be seen as a limitation in this preliminary result. Nevertheless, the preliminary results indicate that going from an EPI- to a spiral-readout may increase the SNR more than going from a 1.5T to a 3T magnetic field strength. This may, for example, allow for acquisition of higher number of time frames without sacrificing SNR. The SNR will mainly effect the precision of the DENSE

measurement.

7.4 Multiple-slice DENSE - Paper IV

The acquisition time of an MRI sequence is often an important factor in clinical applications, as long acquisition times may be tiresome for the patient. In addition, patient with a cardiovascular disease may be anxious about the examination itself and its outcome which may prevent them to relax during the examination. The length of the examination and the stress make the patient more prone to move during the acquisition. Shorter acquisition time may help to increase the compliance of the patient during the examination. Another advantage of short acquisition times is related to the motion caused by breathing. Imaging of the chest is sensitive to the motion caused by the breathing. Different strategies may be used to deal with this motion: data acquisition during breath holds, navigator gating or signal averaging. The choice of strategy is dependent on the application. Breath hold is a common approach for cardiac application with a relatively short acquisition time. This may require a single or multiple breath holds depending on the acquisition time. Cardiovascular patient in general have a reduced capability for holding their breath and may find long and multiple breath hold hard. Long acquisition may therefore be exhausting for them, reduce the compliance of the breath hold regime and consequently affects the data quality acquired. The length of the acquisition is among other dependent on the resolution and the field-of-view of the acquisition. It is also dependent on the number of slices used to cover the heart. Cardiac examinations is commonly using the AHA-standardized 16- and 17-segment models [75]. Traditionally, to acquire DENSE data according to the 16-segment would require three separate acquisitions, one for each of the three slices needed. A multiple-slice DENSE acquisition where the three slices are acquired in the same breath hold would therefore be beneficial for clinical routine.

Several methods exist for accelerated acquisition for MRI in general; SENSE [76], GRAPPA [77], *kt*-BLAST [78] among others. Of these, SENSE has been proposed as a suitable acceleration technique for DENSE [79]. The use of different readout approaches also affects the acquisition time, and other aspects as well. Depending on the acquisition approach, some time in the DENSE acquisition may be spent idle. In Paper IV it is shown that this idle time could be spent measuring other slices. This allows for coverage of all three slices needed for the 16-segment model at the same time previously used to acquire one slice. The multiple-slice approach utilizes that the whole

body is encoded in the initial position encoding preparation in the beginning of the cardiac cycle. The location of the slice selective pulse preceding readout is therefore more or less arbitrary to the initial position encoding. This allows the acquisition of different slices in an interleaved fashion within the same cardiac cycle, which enables the multiple-slice DENSE approach presented in Paper IV. The paper compares the strain acquired with this multiple-slice DENSE with the corresponding 16-segments acquired in three separate single-slice acquisition. The comparison showed good agreement of the strain acquired with the multiple-slice and single slice approach, which implies that the method could be used interchangeable and that the multiple-slice acquisition thus could be used to reduce the acquisition time.

A reflection of multiple-slice technique is that it is dependent on an existing idle time in the intended acquisition. The multiple-slice technique is not as applicable for acquisitions which aim to obtain high temporal resolution as these pulse sequences have very little idle time by design. Other acquisition strategies may also result in less or no idle time, e.g. meta-DENSE.

In a recent abstract, the multiple-slice DENSE approach has been applied to obtain longitudinal strain by acquiring the longitudinal displacement in two adjacent short axis planes [80].

7.5 3D DENSE - Paper V

Physiological research may require detailed analysis covering a large part of the myocardium. These measurements may consequently have to be acquired with a different approach compared to clinical application. Clinical applications is often practically limited in time. Patients may be anxious and find it difficult to remain still during multiple acquisitions. Moreover, a hospital needs to achieve a high throughput of patients, an objective that also limits the examination time for individual patients. However, a physiological study may benefit more by few but more extensively examined volunteers. The acquisition time of these extensive examination may still be acceptable as only a single acquisition is needed compared to the numerous acquisition often required in a clinical examination. DENSE acquisitions are commonly performed in two-dimensional slices, but have also been acquired with three-dimensional acquisition in an intubated and ventilated animal [58].

In Paper V, a navigator-gated three-dimensional DENSE acquisition was used to acquire displacement in the systolic phase and in the diastolic phase of a healthy human heart. The systolic deformation was defined

as the deformation between the R-wave in the ECG and the closure of the aortic valve. For the diastolic phase, on the other hand, two time frames were acquired to obtain the deformation between the time of the mitral valve opening to 75 and 213 ms after the opening. A 3-SPAMM [42] acquisition was used to suppress the FID and the stimulated anti-echo. The combination these three acquisition moreover provided signal averaging for the stimulated echo, but did also increase the acquisition time. To keep the acquisition time within acceptable range, the ECG-triggered measurement consisted of an k-space segment EPI acquisition with SENSE acceleration. As this resulted in an acquisition time in the order of 10 minutes, navigator-gating were used to allow for free-breathing. A balanced multipoint encoding was used for improved SNR and to eliminate direction bias [81]. To produce the same SNR at the two time frames, a variable flip angle approach was used optimized to yield maximum SNR [67, 68]. The displacement data acquired was used to estimate the full strain tensor by using a procedure including segmentation, phase-unwrapping and strain estimation with a polynomial method [82] adapted to three-dimensional DENSE data.

In a recent paper [83], first published online for early view at the time of writing this chapter, a similar approach to acquire the three-dimensional acquisition using DENSE was presented. That acquisition suggested in that paper utilizes a cine spiral readout but was performed without any parallel imaging acceleration technique. In contrast to Paper V, it suggested the use of anisotropic voxels which might make the acquisition more sensitive to signal loss due to shear strain within the voxels and provided a lower spatial resolution, but which on the other hand allows for a greater coverage of the heart within the same acquisition time. The two papers otherwise share several approaches such as navigator-gating, 3-SPAMM, balanced multipoint acquisition and flip angle optimization for constant SNR.

Chapter 8

Discussion

This thesis presents technical evaluations and enhancements of phase based motion sensitive MRI acquisitions, focusing on the accuracy and precision of the acquisition and how acquisition and data analysis can be adapted for clinical and physiology research purposes. The objective of this chapter is to widen the perspective and address some questions that are related more to the research field as a whole.

8.1 Possibilities and hindrances of the phase based motion sensitive methods

Many interesting measures of myocardial deformation can already be acquire adequately with existing applications, such as wall thickening which can be acquired from anatomical imaging by ultrasound or MRI. These measures do, however, not provide a full description of the deformation of the myocardium - an area in which the phase based motion sensitive method can provide additional value. The phase based methods allows for full assessment of the deformation (i.e. measurement of the full strain tensor) on a regional basis (i.e. it allows to resolve the deformation transmurally) and at the same time show promising properties for implementation of user-friendly analysis tools. The detailed analysis these methods enable may therefore reveal alterations in the myocardial function that other methods are unable to study. One area where this detailed analysis of deformation may be favorable is degenerative cardiac diseases. It is not unlikely that the negative remodeling that appears for degenerative diseases influences the characteristics of the regional deformation. Such changes in the characteristics of the deformation have for instance been suggested as an early marker of left ventricular dysfunction [3]. The phase base motion sensitive methods

are probably highly suitable to study these regional deformations, leading to early detection of remodeling. This would enable early treatment and thereby improve quality of life and reduce health care expenses.

However, today, the phase based motion sensitive methods have not become widely used for evaluation of the myocardial function. There are probably a couple of contributing factors for this situation, depending on whether the usage is focused on clinical application or research purposes. Some of these contribution factors are; MRI is not the standard modality for cardiac diagnostics, insufficient evidence of the additional value of the methods, and lack of practical experience.

Firstly, many of the routinely cardiac examinations are performed with ultrasound, and it is unlikely that MRI ever will become the modality that is used to examine the majority of cardiac patients. Ultrasound has in fairness the benefit of being less expensive and it also allows for bedside examinations. Nevertheless, MRI has other advantages that surely give MRI a rightful place as a technique to examine the heart. Some of these advantages are; examination of viability, measurement of volume flow, comprehensive study of complicated geometries, enable multiple contrast settings, allows for the assessment of edema. Accurate acquisition of regional deformation using phase based motion sensitive methods should be considered one of the advantageous areas of MRI as well.

Secondly, the uniquely additional value of the phase based methods has not been proven yet. Evidence of the uniquely additional value can be obtained by demonstrating new advantageous areas rather than pursuing further technical advancement. One such area has already been mentioned; the use of phase based motion sensitive methods for acquisition of regional deformation to find early markers of degenerative cardiac diseases. As these methods lack a suitable golden standard, the evidence of the additional value should relate to how well altered deformation could predict the outcome of the disease or its treatment. After some smaller patient studies, these applications would eventually have to be validated in larger multicenter studies which would require the development of user-friendly toolboxes.

Thirdly, lack of practical experience of using these phase based motion sensitive methods may be a practical hindrance for the usage of the techniques, especially for clinical application, but also for larger research patient studies. Therefore, the methods may not be fully adapted to practical applications. This is probably more related to post processing of the data and user-friendly applications than the acquisition itself. This illuminates the need for technologists and clinicians to work with identifying

and finding solutions to problems that practically limit the applicability of the techniques. Without user-friendly application, large scale studies using phase based motion sensitive methods will become strenuous.

8.2 PC-MRI vs. DENSE

The question of whether PC-MRI or DENSE is the preferred method for the assessment of myocardial function is relatively closely related to the question of whether strain rate or strain is the most suitable measure.

From a clinical perspective, the choice of technique depends on the disease examined - It is not likely that one of the techniques always is the preferable choice. Studies have to determine whether strain rate or strain is the favorable choice in detecting and assessing a certain disease. Changes in the speed of the contraction may be better reflected in the strain rate, while the strain is more affected by changes in the magnitude of the contraction. It is therefore likely that PC-MRI is suitable to detect ischemic diastolic dysfunction, where the lack of oxygen impairs the myocardial relaxation and thereby cause a reduced strain rate. An impaired relaxation does however not have to affect the magnitude of the relaxation, in which case a measurement of the total strain would be unable to detect the disease. For other diseases strain may be an earlier detector than strain rate. This may be the case for ventricular dysfunction in mitral regurgitation. It is not unreasonable to suppose that the remodeling taking place for certain diseases, such as eccentric cardiomyopathy, are related to the elongation of the fibers caused by the extra volume load. Hence, strain rate vs. strain is dependent on the cardiac diseases at hand.

From a technical point of view the acquisition of PC-MRI and DENSE have different properties which may influence its practical usage, both in terms of acquisition and post processing. One of the properties beneficial for DENSE is its inherent black blood effect caused by intravoxel dephasing. This facilitates the distinction of myocardium and blood. PC-MRI may however suffer somewhat from its inherent low contrast between myocardium and blood. This is a potential practical problem in certain cardiac patient, even with the use of saturation pulses that saturate the blood, and may complicate post processing. Another property is the wrapping of the phase which affects both PC-MRI and DENSE. For PC-MRI this problem is avoided by choosing a sufficiently low velocity encoding gradient to prevent ambiguities within the expected range of velocity. In DENSE, these phase wraps are dealt with in the post processing. However, for clinical DENSE application the phase does not have to be unwrapped as strain

can be estimated using only a regional unwrapping, making the problem trivial. For more advanced applications which actually may require unwrapping of the whole myocardium there exist methods which can perform this unwrapping semiautomatically. A third property, which potentially may constitute a limitation for DENSE, is the signal loss caused by tissue deformation during the cardiac cycle [43]. This effect is more pronounced for higher encoding strengths and optimization of the encoding strength in relations to signal strength has been investigated [44]. Certain diseases may however result in increased deformation and thereby increased signal loss. However, this should not constitute any major difficulty, but may require a decreased encoding strength (and thereby slightly reduce the precision for the acquisition) for these diseases.

Strain and strain rate are, as seen in the background, tightly connected. However, the temporal resolution of a practical DENSE acquisition could not be seen as sufficient to estimate strain rate from strain. Estimating strain from PC-MRI is also related with problems. Strain can be estimated from particle traces from the velocity acquired with PC-MRI. However, small inaccuracies in the PC-MRI measurement could accumulate in the tracking process and in the end result in larger inaccuracies in the displacement map. The tracking is also dependant on a sufficient temporal resolution in the velocity data, as too low temporal resolution may prevent the registration of sudden movements. Hence, despite the tight relation between strain and strain rate, these two techniques do in practice acquire complementary information. In conclusion, one of the methods does not exclude the other as both supply unique information of the deformation.

8.3 Clinical routine vs. physiological research

The phase based motion sensitive methods could be used in both clinical routine and physiological research. As suggested earlier in this discussion, these methods will probably not obtain a major clinical breakthrough until it is demonstrated that they provide a unique additional value compared to existing techniques.

Physiological studies using phase based MRI methods may broaden our general knowledge of the myocardial function in health and disease. The cardiac mechanics are often described as complex, and the phase based motion sensitive methods show several advantages which may make it one of the most suitable methods to investigate this complex cardiac kinematics. Some of the most advantageous properties are that it allows for; high resolution, accurate measurement of motion, great freedom to orient imaging

planes or volumes, and it does not require invasive intervention. The resolution of these methods allows to resolve the deformation transmurally and could therefore for instance be used to distinguish the motion endo-, mid- and epicardialy. It provides this resolution in all regions within the heart as it allows for isotropic resolution. This resolution does furthermore not constitute the limit of the accuracy of the measurement as the accuracy is related to the phase of the acquisition and not to the resolution itself. These methods therefore allow for subresolution accuracy. Moreover, as the phase based methods are MRI techniques it allows a great freedom to orient imaging planes or volumes. This is an advantage in comparison to ultrasound, which is limited to certain orientations, and to the surgically implanted markers, which needs to be inserted in advance. The last example of advantageous properties is that these methods do not require invasive intervention. Invasive intervention complicates research studies and may furthermore affect the deformation of the myocardium itself.

The outcome these physiological research using the phase based motion sensitive techniques may lead to better adaption of these techniques to the clinical routine, as the demonstration of unique additional value of these methods and the development of user-friendly applications, as discussed earlier. The obtained knowledge can also be used to improve the assessment by other imaging modalities, such as ultrasound. The phase based methods shows promising features for investigation of the motion and deformation of the myocardium and could therefore be used to find preferable measures for detecting diseases. Rigorous full-scale acquisitions in a minor number of volunteers with a specific disease would allow for the exploration of motion and deformation related to the disease open-mindedly. The findings of such investigations could be used to develop dedicated applications using other highly accessible modalities.

8.4 Future work

The understanding of cardiac physiology and function improves continuously; however, much still remains to be explored, which could lead to better diagnostics and treatment of cardiac disease. Phase based motion sensitive MRI methods show advantageous properties to refine the understanding of the cardiac kinematics. Further work is needed to introduce user-friendly and accessible application of these techniques for both clinical and physiological research purposes. This would facilitate large patient studies; the next step towards clinical application.

Bibliography

- [1] Hill JA, Olson EN. Cardiac plasticity. *N Engl J Med* 2008;358:1370–1380.
- [2] Wandt B, Bojo L, Tolagen K, Wranne B. Echocardiographic assessment of ejection fraction in left ventricular hypertrophy. *Heart* 1999; 82:192–198.
- [3] Carlhäll CJ, Nguyen TC, Itoh A, Ennis DB, Bothe W, Liang D, Ingels NB, Miller DC. Alterations in transmural myocardial strain: an early marker of left ventricular dysfunction in mitral regurgitation? *Circulation* 2008;118:S256–262.
- [4] Hatle L, Angelsen B, Tromsdal A. Noninvasive assessment of atrioventricular pressure half-time by Doppler ultrasound. *Circulation* 1979; 60:1096–1104.
- [5] Miyatake K, Yamagishi M, Tanaka N, Uematsu M, Yamazaki N, Mine Y, Sano A, Hirama M. New method for evaluating left ventricular wall motion by color-coded tissue Doppler imaging: in vitro and in vivo studies. *J Am Coll Cardiol* 1995;25:717–724.
- [6] Leitman M, Lysyansky P, Sidenko S, Shir V, Peleg E, Binenbaum M, Kaluski E, Krakover R, Vered Z. Two-dimensional strain—a novel software for real-time quantitative echocardiographic assessment of myocardial function. *J Am Soc Echocardiogr* 2004;17:1021–1029.
- [7] Spencer A. *Continuum mechanics*. Dover Pubns, 2004.
- [8] Levitt M. *Spin dynamics: basics of nuclear magnetic resonance*. Wiley, 2001.
- [9] Ljunggren S. A simple graphical representation of Fourier-based imaging methods. *Journal of Magnetic Resonance* 1983;54(2):338–343.

-
- [10] Aletras AH, Ding S, Balaban RS, Wen H. DENSE: displacement encoding with stimulated echoes in cardiac functional MRI. *J Magn Reson* 1999;137:247–252.
- [11] Moran PR. A flow velocity zeugmatographic interlace for NMR imaging in humans. *Magn Reson Imaging* 1982;1:197–203.
- [12] Edelman RR, Gaa J, Wedeen VJ, Loh E, Hare JM, Prasad P, Li W. In vivo measurement of water diffusion in the human heart. *Magn Reson Med* 1994;32:423–428.
- [13] Dyverfeldt P, Sigfridsson A, Kvitting JP, Ebberts T. Quantification of intravoxel velocity standard deviation and turbulence intensity by generalizing phase-contrast MRI. *Magn Reson Med* 2006;56:850–858.
- [14] Pelc NJ, Bernstein MA, Shimakawa A, Glover GH. Encoding strategies for three-direction phase-contrast MR imaging of flow. *J Magn Reson Imaging* 1991;1:405–413.
- [15] Dumoulin CL, Souza SP, Darrow RD, Pelc NJ, Adams WJ, Ash SA. Simultaneous acquisition of phase-contrast angiograms and stationary-tissue images with Hadamard encoding of flow-induced phase shifts. *J Magn Reson Imaging* 1991;1:399–404.
- [16] Wigström L, Sjöqvist L, Wranne B. Temporally resolved 3D phase-contrast imaging. *Magn Reson Med* 1996;36:800–803.
- [17] Kozerke S, Hasenkam JM, Pedersen EM, Boesiger P. Visualization of flow patterns distal to aortic valve prostheses in humans using a fast approach for cine 3D velocity mapping. *J Magn Reson Imaging* 2001; 13:690–698.
- [18] Kvitting JP, Ebberts T, Wigström L, Engvall J, Olin CL, Bolger AF. Flow patterns in the aortic root and the aorta studied with time-resolved, 3-dimensional, phase-contrast magnetic resonance imaging: implications for aortic valve-sparing surgery. *J Thorac Cardiovasc Surg* 2004;127:1602–1607.
- [19] Hope TA, Markl M, Wigström L, Alley MT, Miller DC, Herfkens RJ. Comparison of flow patterns in ascending aortic aneurysms and volunteers using four-dimensional magnetic resonance velocity mapping. *J Magn Reson Imaging* 2007;26:1471–1479.

- [20] Hope MD, Meadows AK, Hope TA, Ordovas KG, Saloner D, Reddy GP, Alley MT, Higgins CB. Clinical evaluation of aortic coarctation with 4D flow MR imaging. *J Magn Reson Imaging* 2010;31:711–718.
- [21] Wigström L, Ebberts T, Fyrenius A, Karlsson M, Engvall J, Wranne B, Bolger AF. Particle trace visualization of intracardiac flow using time-resolved 3D phase contrast MRI. *Magn Reson Med* 1999;41:793–799.
- [22] Fyrenius A, Wigström L, Ebberts T, Karlsson M, Engvall J, Bolger AF. Three dimensional flow in the human left atrium. *Heart* 2001; 86:448–455.
- [23] Bolger AF, Heiberg E, Karlsson M, Wigström L, Engvall J, Sigfridsson A, Ebberts T, Kvitting JP, Carlhäll CJ, Wranne B. Transit of blood flow through the human left ventricle mapped by cardiovascular magnetic resonance. *J Cardiovasc Magn Reson* 2007;9:741–747.
- [24] Eriksson J, Carlhäll CJ, Dyverfeldt P, Engvall J, Bolger AF, Ebberts T. Semi-automatic quantification of 4D left ventricular blood flow. *J Cardiovasc Magn Reson* 2010;12:9.
- [25] Zhu Y, Drangova M, Pelc NJ. Fourier tracking of myocardial motion using cine-PC data. *Magn Reson Med* 1996;35:471–480.
- [26] Drangova M, Zhu Y, Pelc NJ. Effect of artifacts due to flowing blood on the reproducibility of phase-contrast measurements of myocardial motion. *J Magn Reson Imaging* 1997;7:664–668.
- [27] Arai AE, Gaither CC, Epstein FH, Balaban RS, Wolff SD. Myocardial velocity gradient imaging by phase contrast MRI with application to regional function in myocardial ischemia. *Magn Reson Med* 1999; 42:98–109.
- [28] Markl M, Schneider B, Hennig J, Peschl S, Winterer J, Krause T, Laubenberger J. Cardiac phase contrast gradient echo MRI: measurement of myocardial wall motion in healthy volunteers and patients. *Int J Card Imaging* 1999;15:441–452.
- [29] Jung B, Schneider B, Markl M, Saurbier B, Geibel A, Hennig J. Measurement of left ventricular velocities: phase contrast MRI velocity mapping versus tissue-doppler-ultrasound in healthy volunteers. *J Cardiovasc Magn Reson* 2004;6:777–783.

- [30] Delfino JG, Bhasin M, Cole R, Eisner RL, Merlino J, Leon AR, Oshinski JN. Comparison of myocardial velocities obtained with magnetic resonance phase velocity mapping and tissue Doppler imaging in normal subjects and patients with left ventricular dyssynchrony. *J Magn Reson Imaging* 2006;24:304–311.
- [31] Kvitting JP, Sigfridsson A, Wigström L, Bolger AF, Karlsson M. Analysis of human myocardial dynamics using virtual markers based on magnetic resonance imaging. *Clin Physiol Funct Imaging* 2010;30:23–29.
- [32] Haase A, Frahm J, Matthaei D, Hanicke W, Bomsdorf H, Kunz D, Tischler R. MR imaging using stimulated echoes (STEAM). *Radiology* 1986;160:787–790.
- [33] Frahm J, Hanicke W, Bruhn H, Gyngell ML, Merboldt KD. High-speed STEAM MRI of the human heart. *Magn Reson Med* 1991;22:133–142.
- [34] Axel L, Dougherty L. MR imaging of motion with spatial modulation of magnetization. *Radiology* 1989;171:841–845.
- [35] Aletras AH, Wen H. Mixed echo train acquisition displacement encoding with stimulated echoes: an optimized DENSE method for in vivo functional imaging of the human heart. *Magn Reson Med* 2001;46:523–534.
- [36] Kim D, Gilson WD, Kramer CM, Epstein FH. Myocardial tissue tracking with two-dimensional cine displacement-encoded MR imaging: development and initial evaluation. *Radiology* 2004;230:862–871.
- [37] Zhong X, Spottiswoode BS, Cowart EA, Gilson WD, Epstein FH. Selective suppression of artifact-generating echoes in cine DENSE using through-plane dephasing. *Magn Reson Med* 2006;56:1126–1131.
- [38] Gilson WD, Yang Z, French BA, Epstein FH. Complementary displacement-encoded MRI for contrast-enhanced infarct detection and quantification of myocardial function in mice. *Magn Reson Med* 2004;51:744–752.
- [39] Epstein FH, Gilson WD. Displacement-encoded cardiac MRI using cosine and sine modulation to eliminate (CANSEL) artifact-generating echoes. *Magn Reson Med* 2004;52:774–781.
- [40] Aletras AH, Arai AE. meta-DENSE complex acquisition for reduced intravoxel dephasing. *J Magn Reson* 2004;169:246–249.

- [41] Axel L, Dougherty L. Heart wall motion: improved method of spatial modulation of magnetization for MR imaging. *Radiology* 1989; 172:349–350.
- [42] Tsao J, Laurent D. N-SPAMM for efficient displacement-encoded acquisition in myocardial tagging. In *Proc. Intl. Soc. Mag. Reson. Med*, volume 13. 2005; 273.
- [43] Fischer SE, Stuber M, Scheidegger MB, Boesiger P. Limitations of stimulated echo acquisition mode (STEAM) techniques in cardiac applications. *Magn Reson Med* 1995;34:80–91.
- [44] Spottiswoode BS, Zhong X, Hess AT, Kramer CM, Meintjes EM, Mayosi BM, Epstein FH. Tracking myocardial motion from cine DENSE images using spatiotemporal phase unwrapping and temporal fitting. *IEEE Trans Med Imaging* 2007;26:15–30.
- [45] Pelc NJ, Herfkens RJ, Shimakawa A, Enzmann DR. Phase contrast cine magnetic resonance imaging. *Magn Reson Q* 1991;7:229–254.
- [46] Hennig J, Schneider B, Peschl S, Markl M, Krause T, Laubenberger J. Analysis of myocardial motion based on velocity measurements with a black blood prepared segmented gradient-echo sequence: methodology and applications to normal volunteers and patients. *J Magn Reson Imaging* 1998;8:868–877.
- [47] Kvitting JP, Ebbers T, Engvall J, Sutherland GR, Wrane B, Wigström L. Three-directional myocardial motion assessed using 3D phase contrast MRI. *J Cardiovasc Magn Reson* 2004;6:627–636.
- [48] Jung B, Zaitsev M, Hennig J, Markl M. Navigator gated high temporal resolution tissue phase mapping of myocardial motion. *Magn Reson Med* 2006;55:937–942.
- [49] Wedeen VJ. Magnetic resonance imaging of myocardial kinematics. Technique to detect, localize, and quantify the strain rates of the active human myocardium. *Magn Reson Med* 1992;27:52–67.
- [50] Selskog P, Heiberg E, Ebbers T, Wigström L, Karlsson M. Kinematics of the heart: strain-rate imaging from time-resolved three-dimensional phase contrast MRI. *IEEE Trans Med Imaging* 2002;21:1105–1109.
- [51] Robson MD, Constable RT. Three-dimensional strain-rate imaging. *Magn Reson Med* 1996;36:537–546.

- [52] Zhu Y, Drangova M, Pelc NJ. Estimation of deformation gradient and strain from cine-PC velocity data. *IEEE Trans Med Imaging* 1997; 16:840–851.
- [53] Bergvall E, Cain P, Arheden H, Sparr G. A fast and highly automated approach to myocardial motion analysis using phase contrast magnetic resonance imaging. *J Magn Reson Imaging* 2006;23:652–661.
- [54] Young AA, Kraitchman DL, Dougherty L, Axel L. Tracking and finite element analysis of stripe deformation in magnetic resonance tagging. *IEEE Trans Med Imaging* 1995;14:413–421.
- [55] Osman NF, Kerwin WS, McVeigh ER, Prince JL. Cardiac motion tracking using CINE harmonic phase (HARP) magnetic resonance imaging. *Magn Reson Med* 1999;42:1048–1060.
- [56] Kuijter JP, Hofman MB, Zwanenburg JJ, Marcus JT, van Rossum AC, Heethaar RM. DENSE and HARP: two views on the same technique of phase-based strain imaging. *J Magn Reson Imaging* 2006;24:1432–1438.
- [57] Ryf S, Spiegel MA, Gerber M, Boesiger P. Myocardial tagging with 3D-CSPAMM. *J Magn Reson Imaging* 2002;16:320–325.
- [58] Rodriguez I, Ennis DB, Wen H. Noninvasive measurement of myocardial tissue volume change during systolic contraction and diastolic relaxation in the canine left ventricle. *Magn Reson Med* 2006;55:484–490.
- [59] Lin AP, Bennett E, Wisk LE, Gharib M, Fraser SE, Wen H. Circumferential strain in the wall of the common carotid artery: comparing displacement-encoded and cine MRI in volunteers. *Magn Reson Med* 2008;60:8–13.
- [60] Soellinger M, Rutz AK, Kozerke S, Boesiger P. 3D cine displacement-encoded MRI of pulsatile brain motion. *Magn Reson Med* 2009;61:153–162.
- [61] Zhong X, Meyer CH, Schlesinger DJ, Sheehan JP, Epstein FH, Larner JM, Benedict SH, Read PW, Sheng K, Cai J. Tracking brain motion during the cardiac cycle using spiral cine-DENSE MRI. *Med Phys* 2009;36:3413–3419.

- [62] Wen H, Bennett E, Epstein N, Plehn J. Magnetic resonance imaging assessment of myocardial elastic modulus and viscosity using displacement imaging and phase-contrast velocity mapping. *Magn Reson Med* 2005;54:538–548.
- [63] Osman NF, Sampath S, Atalar E, Prince JL. Imaging longitudinal cardiac strain on short-axis images using strain-encoded MRI. *Magn Reson Med* 2001;46:324–334.
- [64] Beache GM, Wedeen VJ, Weisskoff RM, O’Gara PT, Poncelet BP, Chesler DA, Brady TJ, Rosen BR, Dinsmore RE. Intramural mechanics in hypertrophic cardiomyopathy: functional mapping with strain-rate MR imaging. *Radiology* 1995;197:117–124.
- [65] Delfino JG, Fornwalt BK, Eisner RL, Leon AR, Oshinski JN. Determination of transmural, endocardial, and epicardial radial strain and strain rate from phase contrast MR velocity data. *J Magn Reson Imaging* 2008;27:522–528.
- [66] Bendel P. Snapshot MRI with T2*-weighted magnetization preparation. *Magn Reson Med* 1993;30:399–402.
- [67] Fischer SE, McKinnon GC, Maier SE, Boesiger P. Improved myocardial tagging contrast. *Magn Reson Med* 1993;30:191–200.
- [68] Stuber M, Spiegel MA, Fischer SE, Scheidegger MB, Danias PG, Pedersen EM, Boesiger P. Single breath-hold slice-following CSPAMM myocardial tagging. *MAGMA* 1999;9:85–91.
- [69] Ryf S, Kozerke S, Spiegel M, Lamerichs R, Boesiger P. Myocardial tagging: comparing imaging at 3.0 T and 1.5 T. In *Proc Intl Soc Magn Reson Med*. 2002; 1675.
- [70] Gutberlet M, Schwinge K, Freyhardt P, Spors B, Grothoff M, Denecke T, Ludemann L, Noeske R, Niendorf T, Felix R. Influence of high magnetic field strengths and parallel acquisition strategies on image quality in cardiac 2D CINE magnetic resonance imaging: comparison of 1.5 T vs. 3.0 T. *Eur Radiol* 2005;15:1586–1597.
- [71] Valeti VU, Chun W, Potter DD, Araoz PA, McGee KP, Glockner JF, Christian TF. Myocardial tagging and strain analysis at 3 Tesla: comparison with 1.5 Tesla imaging. *J Magn Reson Imaging* 2006;23:477–480.

- [72] Markl M, Scherer S, Frydrychowicz A, Burger D, Geibel A, Hennig J. Balanced left ventricular myocardial SSFP-tagging at 1.5T and 3T. *Magn Reson Med* 2008;60:631–639.
- [73] Kellman P, McVeigh ER. Image reconstruction in SNR units: a general method for SNR measurement. *Magn Reson Med* 2005;54:1439–1447.
- [74] Kellman P. Erratum to Kellman P, McVeigh ER. Image reconstruction in SNR units: a general method for SNR measurement. *Magn Reson Med*. 2005;54:1439–1447. *Magn Reson Med* 2007;58:211–212.
- [75] Cerqueira MD, Weissman NJ, Dilsizian V, Jacobs AK, Kaul S, Laskey WK, Pennell DJ, Rumberger JA, Ryan T, Verani MS. Standardized myocardial segmentation and nomenclature for tomographic imaging of the heart. A statement for healthcare professionals from the Cardiac Imaging Committee of the Council on Clinical Cardiology of the American Heart Association. *Int J Cardiovasc Imaging* 2002;18:539–542.
- [76] Pruessmann KP, Weiger M, Scheidegger MB, Boesiger P. SENSE: sensitivity encoding for fast MRI. *Magn Reson Med* 1999;42:952–962.
- [77] Griswold MA, Jakob PM, Heidemann RM, Nittka M, Jellus V, Wang J, Kiefer B, Haase A. Generalized autocalibrating partially parallel acquisitions (GRAPPA). *Magn Reson Med* 2002;47:1202–1210.
- [78] Tsao J, Boesiger P, Pruessmann KP. k-t BLAST and k-t SENSE: dynamic MRI with high frame rate exploiting spatiotemporal correlations. *Magn Reson Med* 2003;50:1031–1042.
- [79] Aletras AH, Ingkanisorn WP, Mancini C, Arai AE. DENSE with SENSE. *J Magn Reson* 2005;176:99–106.
- [80] Chen X, Zhong X, H EF. MRI of Longitudinal Myocardial Strain using Multislice Cine DENSE with Through-plane Displacement Encoding. In *Proceedings of ISMRM*. Stockholm, 2010; .
- [81] Zhong X, Helm PA, Epstein FH. Balanced multipoint displacement encoding for DENSE MRI. *Magn Reson Med* 2009;61:981–988.
- [82] Kindberg K, Karlsson M, Ingels NB, Criscione JC. Nonhomogeneous strain from sparse marker arrays for analysis of transmural myocardial mechanics. *J Biomech Eng* 2007;129:603–610.

- [83] Zhong X, Spottiswoode BS, Meyer CH, Kramer CM, Epstein FH. Imaging three-dimensional myocardial mechanics using navigator-gated volumetric spiral cine DENSE MRI. *Magn Reson Med* 2010; 64:1089–1097.